International Journal of Scientific Research and Engineering Development-– Volume 5 Issue 6, Nov- Dec 2022

Available at www.ijsred.com

RESEARCH ARTICLE OPEN ACCESS

Soret-Dufour Effect on Casson Flow Past Infinite Plate through Porous Medium with Hall Current

A.K. Shukla[*], Santosh Kumar Chauhan[**], Mohammad Suleman Quraishi[***]

[*],[**]Department of Mathematics, RSKD PG College, Jaunpur, U.P., India
ashishshukla1987@gmail.com
[***]Department of Applied Sciences, Jahangirabad Institute of Technology, Barabanki, U.P., India
sulemanformaths86@gmail.com

----------**********----------

Abstract

Shear stress and shear rate have a non-linear relationship that non-Newtonian fluids like Casson fluid can interpret. In the drug and chemical industries, non-Newtonian solutions are employed globally. This investigation of the Soret-Dufour effect on an unsteady MHD Casson fluid flow model with Hall current, viscous dissipation, and radiation absorption across aoscillating vertical plate in porous medium in the presence of radiation and heat generation/absorption is the focus of this research article. For this research, the governing equations of the flow model have been non-dimensionalized, and they have been numerically solved using the Crank-Nicolson implicit finite difference method. Non-dimensional characteristics' influence on velocity profiles, concentration and temperature can be seen bygraphs and tables to study.

Keywords—**Casson Fluid, Viscous dissipation, Magnetohydrodynamics, Hall Current, Soret and Dufour effects.**

----------**********----------

I. INTRODUCTION

Shear stress and shear rate have a non-linear relationship that non-Newtonian fluid can decipher. Worldwide, non-Newtonian solutions are employed in the pharmaceutical and chemical industries as well. Examples include oils, deodorizers, chemicals, syrups, thick drinks, cleansers, and the production of many different colours. In place of ketchup, custard, tooth paste, wheat, paint, blood, and shampoo, there are still a number of polymer liquids and salt explanations that aren't Newtonian fluids. Shear and shear tension are longitudinally correlated in Newtonian fluid. Blood, shampoo, soap, certain oils, jellies, paints, and other different manufacturing & additional technical needs cannot be described as Newtonian fluids. Numerous researchers, programmers, and scientists have studied various uses. Non-Newtonian fluids are much more difficult to investigate than Newtonian fluids, nevertheless. Direct evaluation of non-Newtonian fluid properties using Navier-Stokes equations is not possible.

In the fields of biomechanics and polymer processing, non-Newtonian fluid behaviour is also referred to as the Casson fluid model. Numerous investigations of Non-Newtonian fluid flow

applications filed in the presence of various factors have attracted the attention of numerous mathematicians for many decades. Casson fluid is one of the non-Newtonian fluid types that exhibits elasticity in nature; examples of Casson fluid include honey, jelly, tomato sauce, etc. Casson fluid can also be used to treat human blood. Liaquat Ali Lund et al.[1] is investigated the magnetohydrodynamic (MHD) flow of Casson nanofluid with thermal radiation over an unsteady shrinking surface. Shahanaz Parvin et al.[2] are discussed effects of the mixed convection parameter, concentration buoyancy ratio parameter, Soret–Dufour parameters, and shrinking parameter in MHD Casson fluid flow past shrinking sheet. Lahmaret al.[3] studied heat transfer of squeezing unsteady nanofluid flow under the effects of an inclined magnetic field and variable thermal conductivity. Mohamed R.Eid et al. [4] investigated numerically for Carreau nanofluid flow over a convectively heated nonlinear stretching surface with chemically reactive species. Hammad Alotaibi et al.[5] introduced the effect of heat absorption (generation) and suction (injection) on magnetohydrodynamic (MHD) boundary-layer flow of Casson nanofluid (CNF) via a non-linear stretching surface with the viscous dissipation in two dimensions. Asogwa and Ibe [6] investigated numerical approach of MHD Casson fluid flow over a permeable stretching sheet with heat and mass transfer taking into cognizance the various parameters present. Renuet al.[7] assessed the effect of the inclined outer velocity on heat and flow transportation in boundary layer Casson fluid over a stretching sheet. Ramudu et al. [8] highlighted the impact of magnetohydrodynamic Casson fluid flow across a convective surface with cross diffusion, chemical reaction, non-linear radiative heat. Recently Mahabaleshwar et al.[9] discussed the important roles of SWCNTs and MWCNTs under the effect of magnetohydrodynamics nanofluids flow past over the stretching/shrinking sheet under the repercussions of thermal radiation and Newtonian heating. Ram Prakash Sharma et al. [10] reports MHD Non-Newtonian Fluid Flow past a Stretching Sheet under the Influence of Non-linear Radiation and Viscous Dissipation. Naveed Akbar et al.[11] investigated Numerical Solution of Casson Fluid Flow under Viscous Dissipation and Radiation Phenomenon. Elham Alali et al. [12] studied MHD dissipative Casson nanofluid liquid film flow due to an unsteady stretching sheet with radiation influence and slip velocity phenomenon. T. M. Ajayi et al. [13] have studied Viscous Dissipation Effects on the Motion of Casson Fluid over an Upper Horizontal Thermally Stratified Melting Surface of a Paraboloid of Revolution: Boundary Layer Analysis. N. Pandya and A. K. Shukla [14] have analyzed Effects of Thermophoresis, Dufour, Hall and Radiation on an Unsteady MHD flow past an Inclined Plate with Viscous Dissipation. Rudra Kr. Das and Bhaben Ch. Neog [15] had discussed MHD Flow past a Vertical Oscillating Plate with Radiation and Chemical Reaction in Porous Medium.

In this investigation our aim is to bring to light the effect of unsteady MHD Casson fluid flow through a vertical oscillating plate through porous medium with Soret-Dufour, Hall current, radiation absorption, heat source/sink and first order chemical reaction. The influence of various physical parameters on velocity, temperature and concentration profiles is discussed with the help of tables and graphs. On the other hand important physical quantities like shearing stress, Nusselt number and Sherwood number are discussed through tables.

II. COMPUTATIONAL MODELING OF THE PROBLEM

The unsteady MHD Casson flow of a viscous incompressible electrically conducting fluid past an impulsively/ oscillatory started infinite verticalplate with variable temperature and mass dispersal in the presence of radiation, radiation absorption and Hall

current with viscous dissipation have been considered. The plate is oscillating and vertical in porous medium. The x- axis is taken along the plate and y-axis is taken normal to it. Initially, it is also assumed that the radiation heat flux in x- direction is negligible as compared to that in y -direction. The plate and fluid are at the same temperature and concentration. At time t, the plate is given some impulsive motion along x-direction against gravitational field with constant velocity u_0 , the plate temperature and concentration decrease exponentially with time. The transversely applied magnetic field and magnetic Reynolds number are very small and hence induced magnetic field is minute so it can be considered negligible, Cowling [16]. Due to infinite length in x-direction, the flow variables are functions of y and t only. Under the usual Boussinesq's approximation, governing partial differential equations for this unsteady flow field problem are given by:

A. Continuity equation:

$$\frac{\partial \bar{v}}{\partial \bar{y}} = 0 \quad \Rightarrow \quad \bar{v} = 0 (consider) \quad (1)$$

B. Momentum equation:

$$\frac{\partial \bar{u}}{\partial \bar{t}} = \nu \left(1 + \frac{1}{\lambda}\right) \frac{\partial^2 \bar{u}}{\partial \bar{y}^2} + g\,\beta_t (\bar{T} - \bar{T}_\infty) + g\,\beta_c (\bar{C} - \bar{C}_\infty) - \frac{\sigma B_0{}^2 \sin^2 \eta}{(1 + M_c{}^2)} \bar{u} - \frac{\mu \bar{u}}{\rho_\infty \bar{K}} \quad (2)$$

C. Energy equation:

$$\rho C_p \frac{\partial \bar{T}}{\partial \bar{t}} = k \frac{\partial^2 \bar{T}}{\partial \bar{y}^2} - \frac{\partial q_r}{\partial \bar{y}} + \frac{\rho D_m K_T}{c_s} \frac{\partial^2 \bar{C}}{\partial \bar{y}^2} + \mu \left(\frac{\partial \bar{u}}{\partial \bar{y}}\right)^2 - \bar{Q}_0 (\bar{T} - \bar{T}_\infty) + Q_1 (\bar{C} - \bar{C}_\infty) \quad (3)$$

$$\frac{\partial \bar{C}}{\partial \bar{t}} = D \frac{\partial^2 \bar{C}}{\partial \bar{y}^2} + \frac{D_m K_T}{T_m} \frac{\partial^2 \bar{T}}{\partial \bar{y}^2} - k_r (\bar{C} - \bar{C}_\infty) \quad (4)$$

Where the term $k_r (\bar{C} - \bar{C}_\infty)$ in mass equation for first order chemical reaction, k_r is chemical reaction constant, $\bar{C}$ concentration $\bar{T}$ temperature $\bar{T}_\infty$ temperature of free stream, $\bar{C}_\infty$ concentration of free stream, β is Casson parameter, β_2 is coefficient of volume expansion for mass transfer , β_1 is volumetric coefficient of thermal expansion, T_m mean fluid temperature, q_r radiative heat along y ∗ -axis, $\bar{Q}_0$ coefficient of heat source/sink $\bar{Q}_1$ radiation absorption parameter, ν is kinematic viscosity, $\bar{K}$ is coefficient of permeability of porous medium, D_m is molecular diffusivity, k is thermal conductivity of fluid, C_p denotes specific heat at constant pressure, μ is for viscosity, ρ fluid density, σ electrical conductivity, g is acceleration due to gravity, K_T denotes thermal diffusion ratio and m is Hall current parameter

In Equation 4; $k_r (\bar{C} - \bar{C}_\infty)$ has been taken as first order chemical reaction.

The boundary conditions for this model are assumed as:

$$\left.\begin{array}{lll} \bar{t} \le 0; & \bar{u} = 0, \quad \bar{T} = \bar{T}_\infty, \quad \bar{C} = \bar{C}_\infty & \forall \bar{y} \\ \bar{t} > 0; & \bar{u} = u_0 Cos\omega t, \quad \bar{T} = \bar{T}_\infty + (\bar{T}_w - \bar{T}_\infty) e^{-At}, & \\ & \bar{C} = \bar{C}_\infty + (\bar{C}_w - \bar{C}_\infty) e^{-At} \quad at \quad \bar{y} = 0 & \\ & \bar{u} \to 0, \quad \bar{T} \to \bar{T}_\infty, \quad \bar{C} \to \bar{C}_\infty \quad as\ \bar{y} \to \infty & \end{array}\right\} \quad (5)$$

Where $A = \frac{u_0{}^2}{\nu}$

Roseland explained the term radiative heat flux approximately as

$$q_r = -\frac{4\sigma_{st}}{3a_m}\frac{\partial \bar{T}^4}{\partial \bar{y}^4} \quad (6)$$

Here Stefan Boltzmann constant and absorption coe□cient are σ_{st} and a_m respectively.

In this case temperature di□erences are very-very small within flow, such that $\bar{T}^4$ can be expressed linearly with temperature. It is realized by expanding in a Taylor series about T_∞' and neglecting higher order terms, so

$$\bar{T}^4 \sim= 4\bar{T}_\infty^{\,3}\bar{T} - 3\bar{T}_\infty^{\,4} \quad (7)$$

With the help of equations (6) and (7), we write the equation (3) in this way

$$\rho C_p \frac{\partial \bar{T}}{\partial \bar{t}} = k\frac{\partial^2 \bar{T}}{\partial \bar{y}^2} + \frac{16\bar{T}_\infty^{\,3}\sigma_{st}}{3a_m}\frac{\partial^2 \bar{T}}{\partial \bar{y}^2} + \frac{\rho D_m K_T}{c_s}\frac{\partial^2 \bar{C}}{\partial \bar{y}^2} \quad (8)$$
$$+\mu\left(\frac{\partial \bar{u}}{\partial \bar{y}}\right)^2 - \bar{Q}_0\left(\bar{T}-\bar{T}_\infty\right) + Q_1\left(\bar{C}-\bar{C}_\infty\right)$$

Let us introduce the following dimensionless quantities

$$\left.\begin{aligned}
&u = \frac{\bar{u}}{u_0},\ t = \frac{\bar{t}u_0^{\,2}}{\nu},\ y = \frac{\bar{y}u_0}{\nu},\ \theta = \frac{\bar{T}-\bar{T}_\infty}{\bar{T}_w-\bar{T}_\infty},\\
&C = \frac{\bar{C}-\bar{C}_\infty}{\bar{C}_w-\bar{C}_\infty},\ G_m = \frac{\nu g\beta_c(\bar{C}_w-\bar{C}_\infty)}{u_0^{\,3}},\\
&G_r = \frac{\nu g\beta_t(\bar{T}_w-\bar{T}_\infty)}{u_0^{\,3}},\ K = \frac{u_0^{\,2}}{\nu^2}\bar{K},\ S_c = \frac{\nu}{D}\\
&P_r = \frac{\mu C_p}{k},\quad R = \frac{4\sigma \bar{T}_\infty^{\,3}}{k_m k},\ K_r = \frac{k_r \nu}{u_0^{\,2}},\\
&A = \frac{\nu}{u_0^{\,2}},\ D_u = \frac{D_m K_T(\bar{C}_w-\bar{C}_\infty)}{C_s C_p \nu(\bar{T}_w-\bar{T}_\infty)},\\
&S_r = \frac{D_m K_T(\bar{T}_w-\bar{T}_\infty)}{T_m \nu(\bar{C}_w-\bar{C}_\infty)},\ Q = \frac{Q_0\nu}{\rho C_p u_0^{\,2}}\\
&Q_C = \frac{Q_1\nu(\bar{C}-\bar{C}_\infty)}{\rho c_p u_0^{\,2}(\bar{T}_w-\bar{T}_\infty)},\ E_c = \frac{u_0^{\,2}}{c_p(\bar{T}_w-\bar{T}_\infty)},\\
&M_1 = \frac{M\sin^2\eta}{(1+M_c^{\,2})},\ M = \frac{\sigma B_0^{\,2}\nu}{u_0^{\,2}}
\end{aligned}\right\} \quad (9)$$

Using substitutions of Equation 9, we get non-dimensional form of partial differential Equations 2, 8 and 4 respectively

$$\frac{\partial u}{\partial t} = \left(1+\frac{1}{\lambda}\right)\frac{\partial^2 u}{\partial y^2} + G_r\theta + G_m C - \left(M_1 + \frac{1}{K}\right)u \quad (10)$$

$$\frac{\partial \theta}{\partial t} = \frac{1}{P_r}\left(1+\frac{4R}{3}\right)\frac{\partial^2\theta}{\partial y^2} + D_u\frac{\partial^2 C}{\partial y^2} + Ec\left(\frac{\partial u}{\partial y}\right)^2 \quad (11)$$
$$-Q\theta - Q_C C$$

$$\frac{\partial C}{\partial t} = \frac{1}{S_c}\frac{\partial^2 C}{\partial y^2} + S_r\frac{\partial^2\theta}{\partial y^2} - K_r C \quad (12)$$

With initial and boundary conditions

$$\left.\begin{aligned}
&t \le 0; \quad u = 0, \quad \theta = 0, \quad C = 0 \quad \forall y\\
&t > 0; \quad u = Cos\omega t, \ \theta = e^{-t}, \ C = e^{-t} \ \ at\ y = 0\\
&u \to 0, \quad \theta \to 0, \quad C \to 0 \quad as\ y \to \infty
\end{aligned}\right\} \quad (13)$$

The degree of practical attention include the Skin friction coefficients λ , local Nusselt Nu, and local Sherwood Sh numbers are known as follows:

$$\tau = \left(\frac{\partial u}{\partial y}\right)_{y=0},\ N_u = -\left(\frac{\partial \theta}{\partial y}\right)_{y=0},\ Sh = -\left(\frac{\partial C}{\partial y}\right)_{y=0} \quad (14)$$

III. Mathematical Approach to Solution

Analytical solution of system of partial differential Equations 10, 11 and 12 with boundary conditions given by Equation 13 is not possible. So, these equations, we have used to solve by Crank-Nicolson implicit finite difference method. The Crank-Nicolson finite difference implicit method is a second order method in time ($o(\Delta t^2)$) and space,

hence no restriction on space and time steps, that is, the method is unconditionally stable. The computation is executed for Δy = 0.1, Δt = 0.002 and procedure is repeated till y = 4. Equations 10, 11 and 12 are expressed as

$$\frac{u_{i,j+1}-u_{i,j}}{\Delta t}=$$
$$\left(1+\frac{1}{\lambda}\right)\frac{u_{i-1,j}-2u_{i,j}+u_{i+1,j}+u_{i-1,j+1}-2u_{i,j+1}+u_{i+1,j+1}}{2(\Delta y)^2}$$
$$+G_r\left(\frac{\theta_{i,j+1}+\theta_{i,j}}{2}\right)+G_m\left(\frac{C_{i,j+1}+C_{i,j}}{2}\right)$$
$$-\left(M_1+\frac{1}{K}\right)\left(\frac{u_{i,j+1}+u_{i,j}}{2}\right)$$

(15)

$$\frac{\theta_{i,j+1}-\theta_{i,j}}{\Delta t}=$$
$$\frac{1}{P_r}\left(1+\frac{4R}{3}\right)\left(\frac{\theta_{i-1,j}-2\theta_{i,j}+\theta_{i+1,j}+\theta_{i-1,j+1}-2\theta_{i,j+1}+\theta_{i+1,j+1}}{2(\Delta y)^2}\right)$$
$$+D_u\left(\frac{C_{i-1,j}-2C_{i,j}+C_{i+1,j}+C_{i-1,j+1}-2C_{i,j+1}+C_{i+1,j+1}}{2(\Delta y)^2}\right)$$
$$+E_c\left(\frac{u_{i+1,j}-u_{i,j}}{\Delta y}\right)^2-Q\left(\frac{\theta_{i,j+1}+\theta_{i,j}}{2}\right)-Q_c\left(\frac{C_{i,j+1}+C_{i,j}}{2}\right)$$

(16)

$$\frac{C_{i,j+1}-C_{i,j}}{\Delta t}-\frac{C_{i+1,j}-C_{i,j}}{\Delta y}=$$
$$\frac{1}{S_C}\left(\frac{C_{i-1,j}-2C_{i,j}+C_{i+1,j}+C_{i-1,j+1}-2C_{i,j+1}+C_{i+1,j+1}}{2(\Delta y)^2}\right)$$
$$+S_r\left(\frac{\theta_{i-1,j}-2\theta_{i,j}+\theta_{i+1,j}+\theta_{i-1,j+1}-2\theta_{i,j+1}+\theta_{i+1,j+1}}{2(\Delta y)^2}\right)$$
$$+K_r\left(\frac{C_{i,j+1}+C_{i,j}}{2}\right)$$

(17)

Initial and boundary conditions are also rewritten as:

$$u_{i,0}=0,\qquad \theta_{i,0}=0,\qquad C_{i,0}=0\qquad \forall i$$
$$u_{0,j}=Cos\omega t,\qquad \theta_{0,j}=e^{-j\Delta t},\quad C_{0,j}=e^{-j\Delta t}\quad \forall j$$
$$u_{l,j}\to 0,\qquad \theta_{l,j}\to 0,\qquad C_{l,j}\to 0$$

(18)

Where index i represents to y and j represents to time t, $\Delta t = t_{j+1} - t_j$ and$\Delta y = y_{j+1} - y_j$. Getting the values of u, θ and C at time t, we may compute the values at time t+Δt as following method: we substitute i = 1, 2, ..., l–1 , where n correspond to ∞ ,equations 15 to 17 give tridiagonal system of equations with boundary conditions in equation 18, are solved employing Thomas algorithm as discussed in Carnahan et al.[16], we find values of θ and C for all values of y at t + Δt. Equation 15 is solved by same to substitute these values of θ and C, we get solution for u till desired time t.

IV. Analysis of Results

The present work analyzes the boundary layer unsteady MHD Casson flow past a porous vertical plate with the Soret-Dufour effect with Hall current. The influence of the first order chemical reaction has been incorporated in the mass equation. In order to see a physical view of work, numerical results of velocity profile u, temperature profile θ, concentration profile C have been discussed with the help of graphs and skin friction coefficients, Nusselt number and Sherwood number are discussed with the help of tables. The following values are used for investigation Gr=6.5, Gm=6, K=3, M=5.5, Mc=0.5, Pr=0.7, Du=0.1, Sc=0.6, Sr=4, R=5, Q=4, Ec=3.5, Q_c=4, Kr=3, λ=0.2, ω=$\pi/3$. It is noted from figure 2 that increasing radiation parameter R, velocity u

increases. This is correct observation because the increase in radiation reveals heat energy to flow. Figure 19 depicts the importance of radiation on temperature distribution. It is analyzed that an increase in R, temperature θ increases and it is notable that an increase in R, concentration C near to plate slightly increases after that decrease in figure 23. In figure 5, velocity decreases as Prandtl number Pr increases and temperature first slightly increases and then decreases rapidly in figure 15 when Pr increases. In figure 26 concentration C near to plate decreases and some distance from plate concentration increases as Prandtl number increases. Figure 22 depicts the variation of Schmidt number Sc as concentration decreases rapidly with increase Sc while it is noteworthy that on increasing Schmidt numbers Sc velocity profile in figure 8 slightly decreases near to plate. In figure 7 and 18, it is seen that velocity and temperature slightly increases as increase Dufour number Du. In figure 9, 21 and 28, it is seen that velocity and temperature slightly increases and concentration increases rapidly as increase in Soret number Sr. Figures 6 and 27 depict the behavior of chemical reaction parameter Kr on velocity and concentration respectively. It is seen that velocity slightly increases and concentration decreases rapidly as Kr increase. It is observe that on increasing Casson parameter λ, velocity profile slightly increases and decreases in Figure 11. Figure 10 reveals that velocity increases on increase of porosity parameter K. The negative value of $Q < 0$ means heat absorption and the positive value of $Q > 0$ means heat transfer. In figure 3 and 12, velocity profile decreases on increasing heat source/sink parameter Q and magnetic parameter M while in figure 13 velocity increase on increase of hall parameter $M_c$and also reducing momentum boundary layer. Figure 14 shows decrement of velocity on increasing oscillation parameter ω. Figure 17 analyzed the impact of heat source/sink parameter Q in the temperature profile. It can be seen that the temperature profile decreases rapidly and the thermal boundary layer reduces for an increase of heat source parameter but it increases with the heat sink parameter. Figure 25, depicts that concentration profile increases on an increase of heat source/sink parameter. The influence of Radiation absorption parameter Q_c on the velocity, temperature and concentration profiles in figure 4, 16 and figure 24 have been shown. We observe that when on increasing Q_c results in the concentration profile also decreases while velocity and temperature increases. Figure 1, 20 and 29 reveals that velocity increases rapidly, temperature interestingly decreases and increases while concentration slightly decreases and increase on increase of time.

V. Conclusions

Effect of viscous dissipation, first order chemical reaction, change in Soret-Dufour and Hall current effects on unsteady MHD flow past a vertical oscillating plate in a porous medium are analyzed. This investigation the following conclusions have come:

The effect of radiation on concentration is noteworthy. It is observed that increasing values of R, concentration goes up and after some distance from the plate, it goes down slowly-slowly.

Interestingly, the change in concentration has been found first decreases then increases on increasing Prandtl number P r and reverse action in case of temperature profile. Velocity profile decreases.

Increasing values of Dufour number, it is observed that velocity and temperature profile in the thermal boundary layer increases in the boundary layer.

Schmidt number greatly influences the concentration profile in the concentration boundary layer.

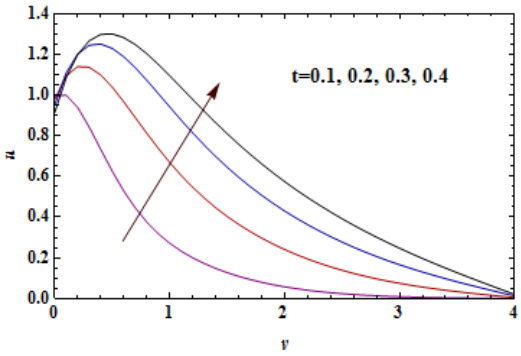

Figure. 1 Velocity Profiles for Different Values of t

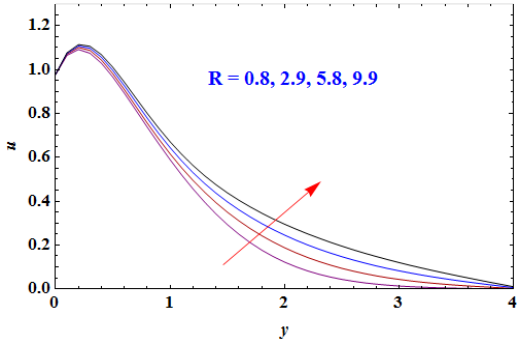

Figure. 2 Velocity Profiles for Different Values of R

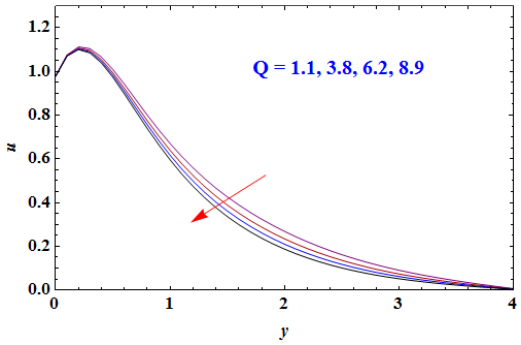

Figure. 3 Velocity Profiles for Different Values of Q

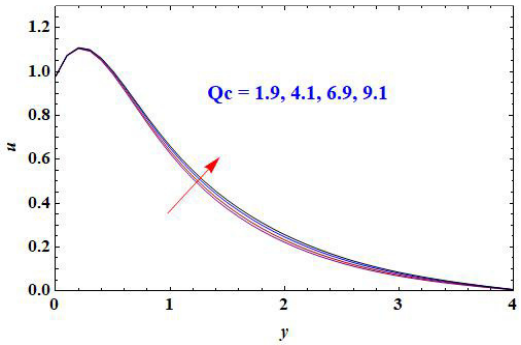

Figure. 4 Velocity Profiles for Different Values of Qc

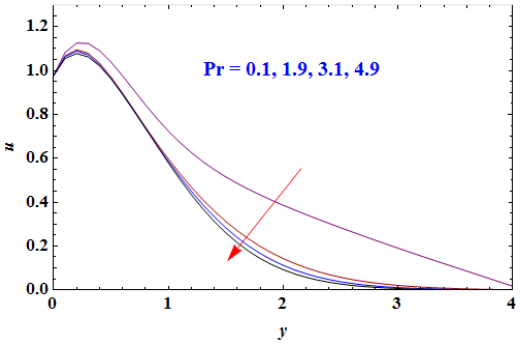

Figure. 5 Velocity Profiles for Different Values of Pr

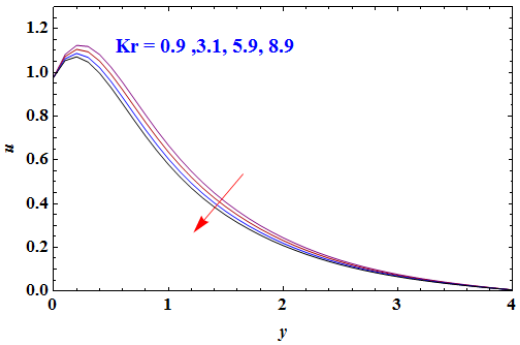

Figure. 6 Velocity Profiles for Different Values of Kr

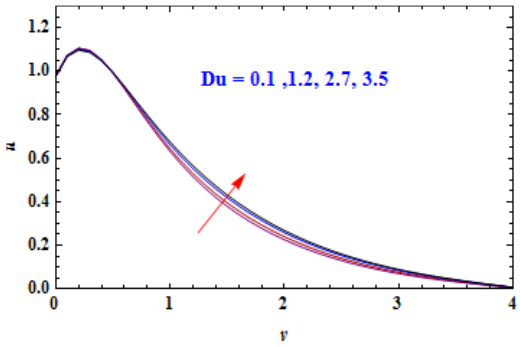

Fig. 7 Velocity Profiles for Different Values of Du

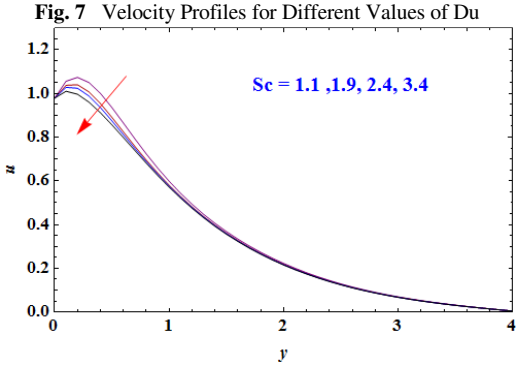

Figure. 8 Velocity Profiles for Different Values of Sc

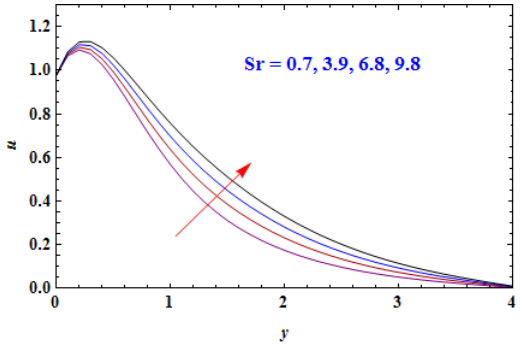

Fig. 9 Velocity Profiles for Different Values of Sr

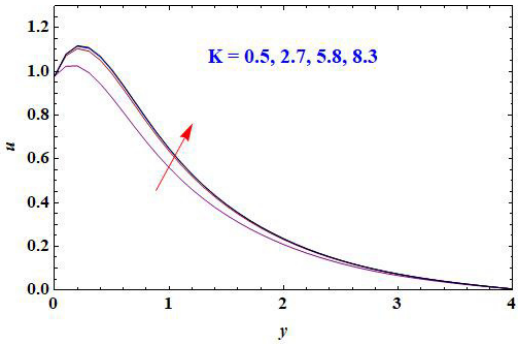

Fig. 10 Velocity Profiles for Different Values of K

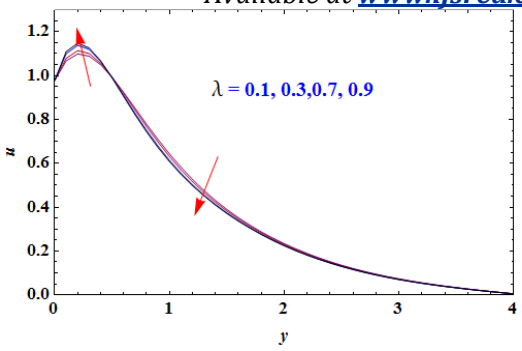

Figure. 11 Velocity Profiles for Different Values of λ

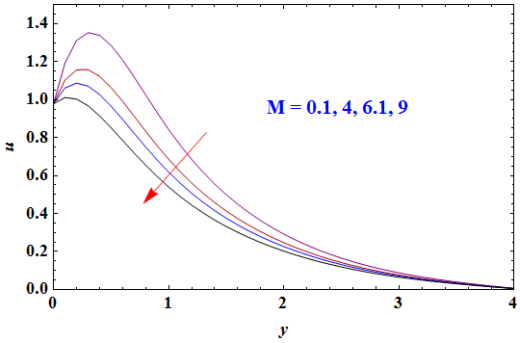

Fig. 12 Velocity Profiles for Different Values of M

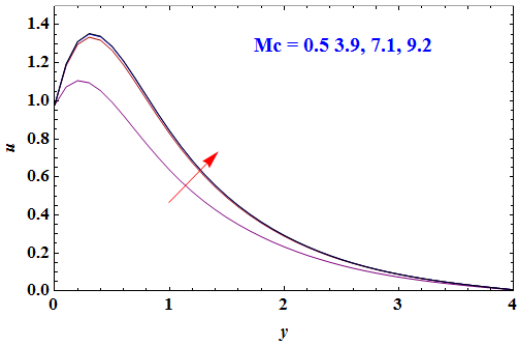

Fig. 13 Velocity Profiles for Different Values of Mc

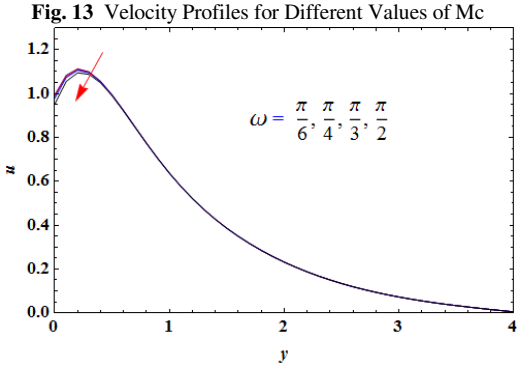

Fig. 14 Velocity Profiles for Different Values of ω

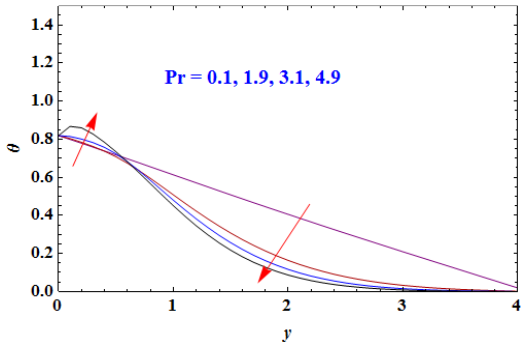

Fig. 15 Temperature Profiles for Different Values of Pr

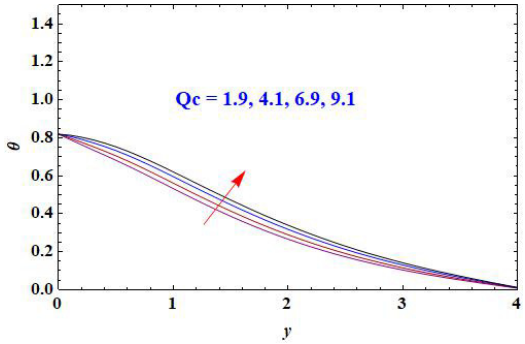

Fig. 16 Temperature Profiles for Different Values of Qc

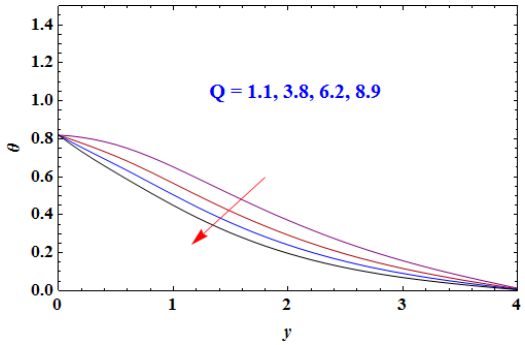

Fig. 17 Temperature Profiles for Different Values of Q

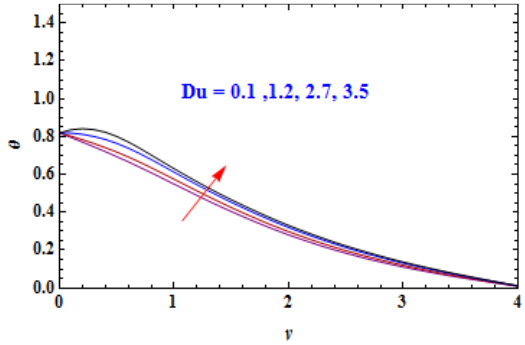

Fig. 18 Temperature Profiles for Different Values of Du

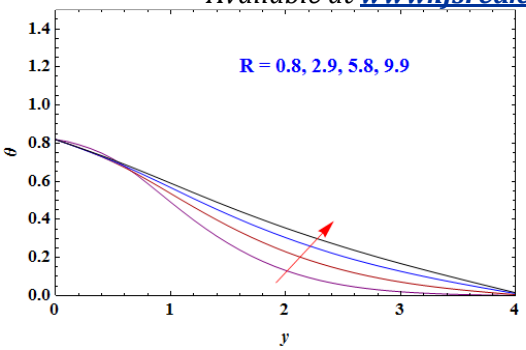

Fig. 19 Temperature Profiles for Different Values of R

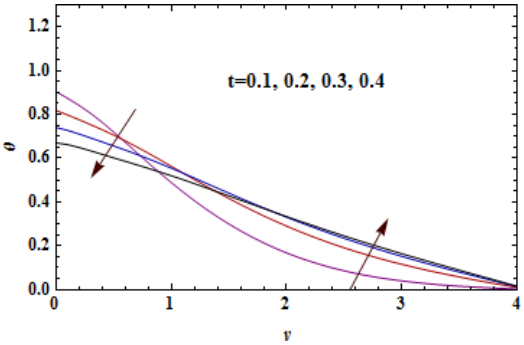

Fig. 20 Temperature Profiles for Different Values of t

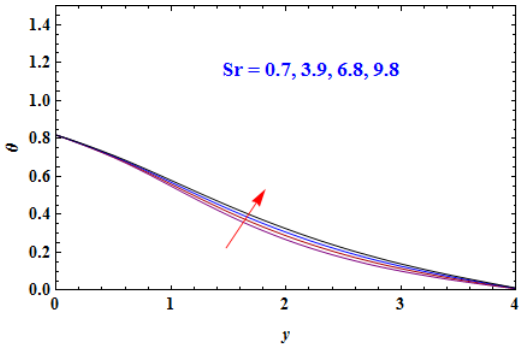

Fig. 21 Temperature Profiles for Different Values of Sr

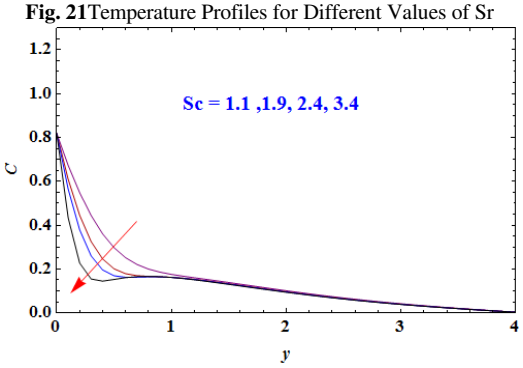

Fig. 22 Concentration Profiles for Different Values of Sc

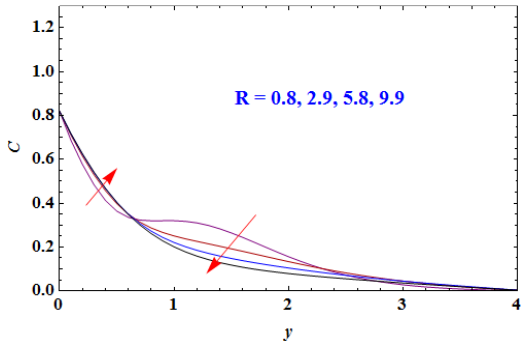

Fig. 23 Concentration Profiles for Different Values of R

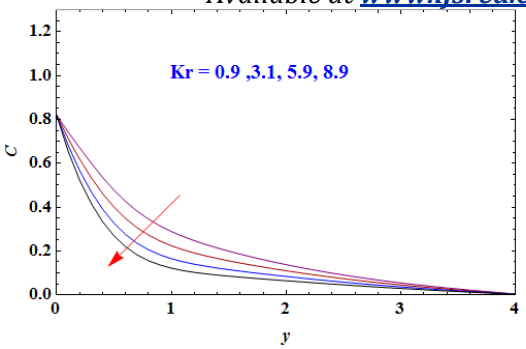

Fig. 27 Concentration Profiles for Different Values of Kr

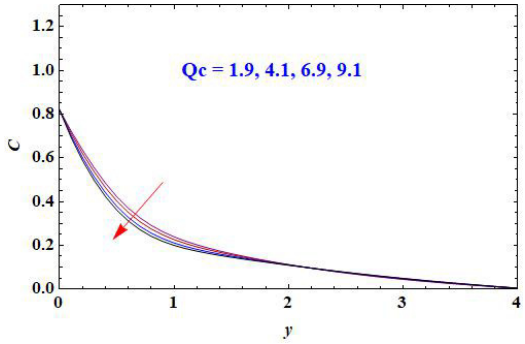

Fig. 24 Concentration Profiles for Different Values of Qc

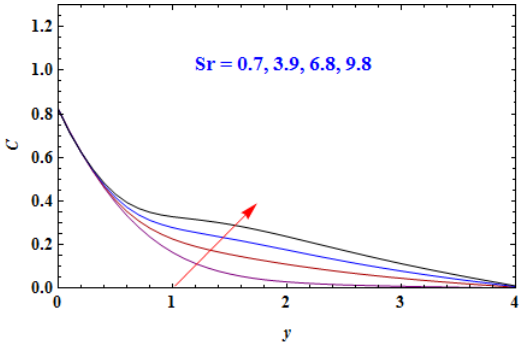

Fig. 28 Concentration Profiles for Different Values of Sr

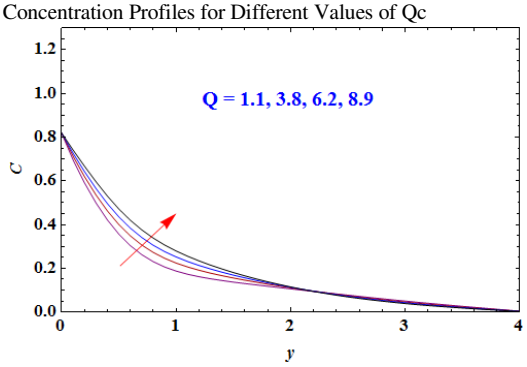

Fig. 25 Concentration Profiles for Different Values of Q

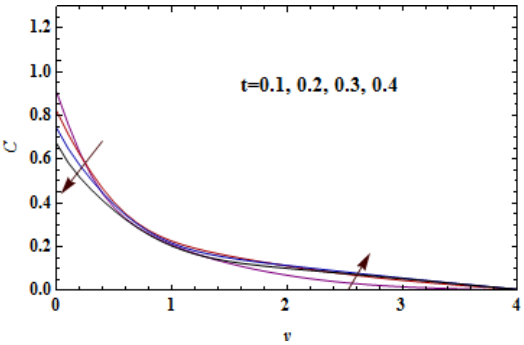

Fig. 29 Concentration Profiles for Different Values of 't'

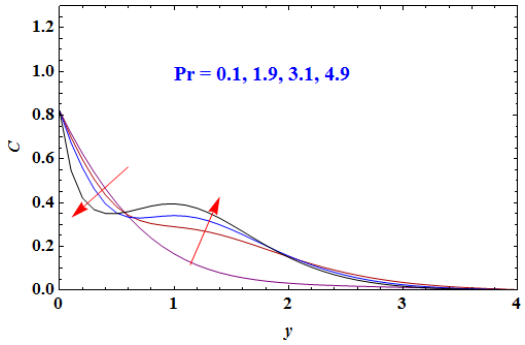

Fig. 26 Concentration Profiles for Different Values of Pr

Table 1.
Skin friction coefficient τ, Nusselt number Nu and Sherwood number Sh for different values of parameters

Q	Q_c	M	Mc	Pr	Sr	R	Kr	ω	K	Du	t	τ	Nu	Sh
1.1	4	5.5	0.5	0.7	4	5	3	3	3	0.6	0.2	0.977083	0.037415	1.22171
3.8	4	5.5	0.5	0.7	4	5	3	3	3	0.6	0.2	0.951478	0.198162	1.05695
6.2	4	5.5	0.5	0.7	4	5	3	3	3	0.6	0.2	0.934331	0.320605	0.919792
8.9	4	5.5	0.5	0.7	4	5	3	3	3	0.6	0.2	0.919865	0.440997	0.774366
4	1.9	5.5	0.5	0.7	4	5	3	3	3	0.6	0.2	0.944093	0.278952	3.954447
4	4.1	5.5	0.5	0.7	4	5	3	3	3	0.6	0.2	0.950134	0.205788	1.04943
4	6.9	5.5	0.5	0.7	4	5	3	3	3	0.6	0.2	0.957302	0.118599	1.16438
4	9.1	5.5	0.5	0.7	4	5	3	3	3	0.6	0.2	0.962554	0.054392	1.25033
4	4	0.1	0.5	0.7	4	5	3	3	3	0.6	0.2	2.15469	0.141279	1.12191
4	4	4	0.5	0.7	4	5	3	3	3	0.6	0.2	1.25073	0.198422	1.05448
4	4	6.1	0.5	0.7	4	5	3	3	3	0.6	0.2	0.835788	0.212039	1.04328
4	4	9	0.5	0.7	4	5	3	3	3	0.6	0.2	0.329253	0.219279	1.04462
4	4	5.5	0.5	0.7	4	5	3	3	3	0.6	0.2	0.949867	0.209022	1.04521
4	4	5.5	3.9	0.7	4	5	3	3	3	0.6	0.2	2.07197	0.148193	1.11313
4	4	5.5	7.1	0.7	4	5	3	3	3	0.6	0.2	2.14601	0.142021	1.12096
4	4	5.5	9.2	0.7	4	5	3	3	3	0.6	0.2	2.15977	0.140843	1.2246
4	4	5.5	0.5	0.1	4	5	3	3	3	0.6	0.2	1.04763	0.199763	1.01792
4	4	5.5	0.5	1.9	4	5	3	3	3	0.6	0.2	0.891025	0.155251	1.2014
4	4	5.5	0.5	3.4	4	5	3	3	3	0.6	0.2	0.85697	0.047424	1.44785
4	4	5.5	0.5	4.9	4	5	3	3	3	0.6	0.2	0.776379	-0.4842	2.71546
4	4	5.5	0.5	0.7	0.7	5	3	3	3	0.6	0.2	0.887822	0.216566	1.02754
4	4	5.5	0.5	0.7	3.9	5	3	3	3	0.6	0.2	0.947927	0.209287	1.04471
4	4	5.5	0.5	0.7	6.8	5	3	3	3	0.6	0.2	1.00541	0.200712	1.0603
4	4	5.5	0.5	0.7	9.8	5	3	3	3	0.6	0.2	1.06681	0.189805	1.8392
4	4	5.5	0.5	0.7	4	0.8	3	3	3	0.6	0.2	0.870925	0.099298	1.32932
4	4	5.5	0.5	0.7	4	2.9	3	3	3	0.6	0.2	0.922508	0.19969	1.08895
4	4	5.5	0.5	0.7	4	5.8	3	3	3	0.6	0.2	0.958046	0.208859	1.03751
4	4	5.5	0.5	0.7	4	9.9	3	3	3	0.6	0.2	0.988913	0.20337	1.02106
4	4	5.5	0.5	0.7	4	5	0.9	3	3	0.6	0.2	1.04076	0.204977	0.755402
4	4	5.5	0.5	0.7	4	5	3.1	3	3	0.6	0.2	0.945918	0.209164	1.05774
4	4	5.5	0.5	0.7	4	5	5.9	3	3	0.6	0.2	0.847045	0.211696	1.37055
4	4	5.5	0.5	0.7	4	5	8.9	3	3	0.6	0.2	0.761635	0.212193	1.64139
4	4	5.5	0.5	0.7	4	5	3	6	3	0.6	0.2	0.893335	0.208493	1.04561
4	4	5.5	0.5	0.7	4	5	3	4	3	0.6	0.2	0.916937	0.20873	1.04541
4	4	5.5	0.5	0.7	4	5	3	3	3	0.6	0.2	0.949867	0.209022	1.04521
4	4	5.5	0.5	0.7	4	5	3	2	3	0.6	0.2	1.04324	0.209615	1.045
4	4	5.5	0.5	0.7	4	5	3	3	0.5	0.6	0.2	0.458711	0.218339	1.04281
4	4	5.5	0.5	0.7	4	5	3	3	2.7	0.6	0.2	0.93822	0.209355	1.04497
4	4	5.5	0.5	0.7	4	5	3	3	5.8	0.6	0.2	1.00089	0.207498	1.04635
4	4	5.5	0.5	0.7	4	5	3	3	8.3	0.6	0.2	1.0175	0.206978	1.04675
4	4	5.5	0.5	0.7	4	5	3	3	3	0.1	0.2	0.95094	0.238521	0.996369
4	4	5.5	0.5	0.7	4	5	3	3	3	1.2	0.2	0.947112	0.167246	1.11692
4	4	5.5	0.5	0.7	4	5	3	3	3	2.7	0.2	0.926869	0.004508	1.42057
4	4	5.5	0.5	0.7	4	5	3	3	3	3.5	0.2	0.896739	-0.17454	1.78749
4	4	5.5	0.5	0.7	4	5	3	3	3	0.6	0.1	0.046976	0.300524	1.45953
4	4	5.5	0.5	0.7	4	5	3	3	3	0.6	0.2	1.14786	0.202488	1.05061
4	4	5.5	0.5	0.7	4	5	3	3	3	0.6	0.3	1.56445	0.128189	0.92602
4	4	5.5	0.5	0.7	4	5	3	3	3	0.6	0.4	1.71416	0.077557	0.864342

REFERENCES

[1] Shafiq A., Rasool G. and Tlili I. (2020), "Marangoni convective nanofluid flow over an electromagnetic actuator in the presence of first-order chemical reaction" Heat Transf. Asian Res /Vol.49/ Pp. 274–288.

[2] Parvin S.; Mohamed Isa S.S.P., Arifin, N.M., Md Ali, F. (2021), "The Inclined Factors of Magnetic Field and Shrinking Sheet in Casson Fluid Flow, Heat and Mass Transfer Symmetry"/Vol.13/ No.373, https://doi.org/10.3390/ sym13030373.

[3] LahmarSihem, Kezzar Mohamed, Eid Mohamed R., and Sari, Mohamed Rafik (2020), "Heat transfer of squeezing unsteady nanofluid flow under the effects of an inclined magnetic field and variable thermal conductivity" Physica A: Statistical Mechanics and its Applications, Elsevier / Vol. 540(C).

[4] M. R. Eid, K. Mahny, A. Dar and T. Muhammad (2020), "Numerical study for Carreau nanofluid flow over aconvectively heated nonlinear stretching surface with chemically reactive species" Physica A: Statistical Mechanics and Its Applications /Vol. 540/ 123063.

[5] Hammad Alotaibi, Saeed Althubiti, Mohamed R. Eid, K. L. Mahny (2021), "Numerical Treatment of MHD Flow of Casson Nanofluid via Convectively Heated Non-Linear Extending Surface with Viscous Dissipation and Suction/Injection Effects" /Vol. 66/ No.1, Pp. 229-245, doi:10.32604/cmc.2020.012234.

[6] K. K. Asogwa and A. A. Ibe, (2020), "A Study of MHD Casson Fluid Flow over a Permeable Stretching Sheet with Heat and Mass Transfer" Journal of Engineering Research and Reports /Vol. 16/ No.2, Pp. 10-25.

[7] Renu Devi, Vikas Poply, Manimala (2021), "Effect of aligned magnetic field and inclined outer velocity in casson fluid flow over a stretching sheet with heat source" Journal of Thermal Engineering /Vol.7/ No.4, Pp. 823-844.

[8] K Kumar Anantha, ,AnkalagiriRamuduSugunammaVangala, Dr.N. Sandeep (2021), "Impact of Soret and Dufour on MHD Casson fluid flow past a stretching surface with convective-diffusive conditions" Journal of Thermal Analysis and Calorimetry 10.1007/s10973-021-10569-w.

[9] U. S. Mahabaleshwar, K. N. Sneha, Akio Miyara, M. Hatami (2022), "Radiation effect on inclined MHD flow past a super-linear stretching/shrinking sheet including CNTs, Waves in Random and Complex Media" DOI: 10.1080/17455030.2022.2053238.

[10] Ram Prakash Sharma and Sachin Shaw (2022), "MHD Non-Newtonian Fluid Flow past a Stretching Sheet under the Influence of Non-linear Radiation and Viscous Dissipation" J. Appl. Comput. Mech. /Vol. 8/ No. 3, Pp. 949-961.

[11] Naveed Akbar, Sardar Muhammad Hussain and Riaz Ullah Khan (2022), "Numerical Solution of Casson Fluid Flow under Viscous Dissipation and Radiation Phenomenon" Journal of Applied Mathematics and Physics /Vol. 10/ Pp. 475-490.

[12] Elham Alali Elham Alali and Ahmed M. Megahed (2022), "MHD dissipative Casson nanofluid liquid film flow due to an unsteady stretching sheet with radiation influence and slip velocity phenomenon" Nanotechnology Reviews/ Vol. 11/ Pp. 463–472

[13] T. M. Ajayi, A. J. Omowaye, and I. L. Animasaun(2017), "Viscous Dissipation Effects on the Motion of Casson Fluid over an Upper Horizontal Thermally Stratified Melting Surface of a Paraboloid of Revolution: Boundary Layer Analysis" Hindawi Journal of Applied Mathematics /Vol. 2017/ https://doi.org/10.1155/2017/1697135.

[14] N. Pandya and A. K. Shukla (2014), "Effects of Thermophoresis, Dufour, Hall and Radiation on an Unsteady MHD flow past an Inclined Plate with Viscous Dissipation" International Journal of Mathematics and Scientific Computing /Vol. 4/ No. 2.

[15] Rudra Kr. Das and Bhaben Ch. Neog (2015), "MHD Flow past a Vertical Oscillating Plate with Radiation and Chemical Reaction in Porous Medium", IOSR Journal of Mathematics, /Vol 11/ No.1/Pp 46-50.

[16] Brice Carnahan, H.A. Luther and James O. Wilkes. (1990), Applied Numerical Methods, Krieger Pub Co, Florida.

[17] T. G. Cowling (1990), Magneto-Hydrodynamics, Inter Science Publishers, New York.

